# Electron collisions with the diatomic fluorine anion

H. B. Pedersen,* R. Bilodeau,† M. J. Jensen, I. V. Makassiouk,‡ C. P. Safvan,§ and L. H. Andersen
*Institute of Physics and Astronomy, University of Aarhus, DK-8000 Aarhus C, Denmark*
(Received 6 June 2000; published 15 February 2001)

Collisions between free electrons and the molecular anion $F_2^-$ have been studied in a merged beams experiment at the heavy ion storage ring ASTRID. Absolute cross sections for detachment ($e^- + F_2^- \rightarrow F_2^0 + 2e^-$ or $F^0 + F^0 + 2e^-$) and dissociation ($e^- + F_2^- \rightarrow F^0 + F^- + 2e^-$) are reported in the energy range 0–27 eV. Branching ratios between the two detachment channels are also given. Dissociation is found to be the dominating reaction and the dissociation cross section is about an order of magnitude larger than the detachment cross section in the investigated energy range. The threshold for detachment is as high as 10 eV, and the branching into the channel with a molecular fragment amounts to less than 20% over most of the energy range. The results are compared to previously measured cross sections for other anions and the importance of nuclear dynamics in the processes is discussed.

DOI: 10.1103/PhysRevA.63.032718 PACS number(s): 34.80.Kw

## I. INTRODUCTION

Electron-impact detachment from atomic anions has been studied both experimentally [1–13] and theoretically [14–23] and an understanding of the dynamics of this process is emerging. The corresponding reactions in collisions between free electrons and molecular anions have been investigated in a series of experiments at the ASTRID (Aarhus Storage Ring Denmark) heavy ion storage ring [24–26]. The physics of electron-anion reactions for molecular systems is different from the atomic ones in several respects. The electronic structure is generally more complex and the coupling to the nuclear motion leading to rovibrational excitation or dissociation adds a new aspect to the reaction dynamics.

In this paper, we report on measurements of the cross sections for three processes

$$e^- + F_2^- \rightarrow \begin{cases} F_2^0 + 2e^- \\ F^0 + F^0 + 2e^- \\ F^0 + F^- + e^- \end{cases} \quad (1)$$

resulting from collisions between free electrons and $F_2^-$ for relative energies in the range 0–27 eV. The first two reactions involve electron detachment leading either to a neutral molecule ($F_2^0$) in a pure *detachment* reaction or to two neutral atoms ($F^0 + F^0$) in a *detachment plus dissociation* reaction. The last reaction is *dissociation*.

The study of these processes for $F_2^-$ completes a systematic investigation of electron-anion reactions at low energy for stable homonuclear molecular anions of the first row elements [26]. The systematic investigation aims at clarifying the general features of electron-anion collisions, such as threshold behaviors and reaction mechanisms. In Table I, we summarize some of the known structural parameters for the neutral and anionic systems. Both the electronic and the nuclear structure of the neutral and anionic systems change systematically for this series of molecular systems. Within the independent particle model, molecular orbitals resulting from linear combinations of atomic *p* orbitals are populated. Along the sequence, the outermost electrons occupy either bonding ($3\sigma_g^+$ and $1\pi_u$) or antibonding ($3\sigma_u^+$ and $1\pi_g$) electronic orbitals. Also, the overlap between the nuclear wave functions in the anion and neutral states varies for these diatomic molecules, which is directly reflected in the equilibrium distances and fundamental vibrational frequencies. Similarly, the overall strength of the electronic binding changes, having a maximum where the binding orbitals are filled, as is the case for $C_2^-$.

With the study of $e^- + F_2^-$ collisions, we wish to further clarify the dynamics of electron-anion reactions. The potential-energy curves for the energetically lowest states of $F_2^-$ and the ground state of $F_2^0$ are shown in Fig. 1 [34]. Two features are unique for $F_2^-$ compared to the previously studied systems. Firstly, the electron affinity EA of $F_2^0$ is larger than the dissociation energy of $F_2^-$, $EA(F_2^0) > D_e(F_2^-)$. Secondly, the equilibrium distances of the ground states of $F_2^0$ and $F_2^-$ are very different, $r_e(F_2^-) - r_e(F_2^0) = 0.5$ Å. Assuming the electron-anion reaction proceeds primarily by vertical transitions, the neutral and anionic systems are effectively separated at low energy, i.e., autodetachment from the repulsive states ($^2\Pi_g$, $^2\Pi_u$, $^2\Sigma_g^+$) of $F_2^-$ to the ground state of $F_2^0$ is hindered energetically below the $X\,^1\Sigma_g^+$ state of $F_2^0$, and above this state there is a poor overlap of the nuclear wave functions of the $X\,^2\Sigma_u^+$ ground state of $F_2^-$ and the autodetaching repulsive curves of $F_2^-$. In the previously studied systems, the significance of electronic excitation prior to intrinsic rearrangement was unclarified.

*Present address: The Weizmann Institute of Science, Rehovot 76100, Israel.

†Present address: McMaster University, Hamilton, Ontario, Canada L84 4M1.

‡Present address: Department of Physics, St. Petersburg State Mining Institute (Technical University), 21 Liniya VO, 2. 199026 St. Petersburg, Russia.

§Present address: Nuclear Science Center, P.O. Box 10502, Aruna Asaf Ali Marg, New Delhi 110067, India.

 ©2001 The American Physical Society

TABLE I. Structural parameters for the homonuclear diatomic molecules of the first row elements.

| Molecule | Ground state | Electron configuration | $r_e$ (Å) | $\omega_e$ ($cm^{-1}$) | $D_e$ (eV) | EA (eV) | Ref. |
|---|---|---|---|---|---|---|---|
| $B_2^0$ | $^3\Sigma_g^-$ | $\ldots(1\pi_u)^2$ | 1.59 | 1051.3 | 3.1 | 2.00[a] | [27,28] |
| $B_2^-$ | $^4\Sigma_g^-$ | $\ldots(1\pi_u)^2(3\sigma_g^+)$ | 1.63[a] | 1010[a] | 4.21[a] | | [28] |
| $C_2^0$ | $^1\Sigma_g^+$ | $\ldots(1\pi_u)^4$ | 1.243 | 1855 | 6.32 | 3.27 | [27] |
| $C_2^-$ | $^2\Sigma_g^+$ | $\ldots(1\pi_u)^4(3\sigma_g^+)$ | 1.268 | 1781.20 | 8.45 | | [29] |
| $O_2^0$ | $^3\Sigma_g^-$ | $\ldots(1\pi_u)^4(3\sigma_g^+)^2(1\pi_g)^2$ | 1.208 | 1580 | 5.214 | 0.39 | [30–33] |
| $O_2^-$ | $^2\Pi_g$ | $\ldots(1\pi_u)^4(3\sigma_g^+)^2(1\pi_g)^3$ | 1.341 | 1089 | 4.23 | | [32] |
| $F_2^0$ | $^1\Sigma_g^+$ | $\ldots(1\pi_u)^4(3\sigma_g^+)^2(1\pi_g)^4$ | 1.42[a] | 892[a] | 1.63[a] | 3.10 | [34] |
| $F_2^-$ | $^2\Sigma_u^+$ | $\ldots(1\pi_u)^4(3\sigma_g^+)^2(1\pi_g)^4(3\sigma_u^+)$ | 1.92 | 462 | 1.26 | | [34] |

[a]*Ab initio* calculation.

## II. EXPERIMENT

The experiment was carried out at the heavy ion storage ring ASTRID [36]. The ring is 40 m in perimeter, and has a square geometry with two 45° bending magnets in each of the four corners. A schematic drawing of the storage ring is shown in Fig. 2. A beam of ~35 nA of $F_2^-$ at 150 keV was extracted from a sputter ion source [37] with a sputtering material made of 50% LiF and 50% Cu powder. This ion beam was injected into the storage ring and further accelerated to 2.486 MeV by means of a radio-frequency acceleration system. After acceleration the ion current was typically ~25 nA. The residual gas pressure in the ring was $\sim 3\times10^{-11}$ mbar resulting in a storage lifetime of 1.3 s. The accelerated ion beam was merged with an essentially monoenergetic electron beam provided by the electron cooler [13,38]. The electron current was 0.3 mA at the cooling energy defined from the matching velocity of ions and electrons. The electron cooler was operated in a chopping mode. Thus, the electron beam was alternatingly turned on and off at a frequency of 20 Hz, and the data acquisition system was gated to measure the rate of collision fragments with the electron beam on and off accordingly.

Neutral particles ($F_2^0$, $F^0$) produced in the electron-ion collision process were detected by a $60\times40$ mm$^2$ energy-sensitive surface barrier detector located behind the dipole magnet following the electron cooler. Grids with transmissions $T_1=67\pm3\%$ and $T_2=23\pm3\%$ were inserted in front of this detector to measure the branching ratio of detachment and detachment plus dissociation. A horizontally movable 20-mm diameter surface barrier detector was positioned inside the first 45° bending magnet following the electron cooler. With this detector, $F^-$ particles originating from the

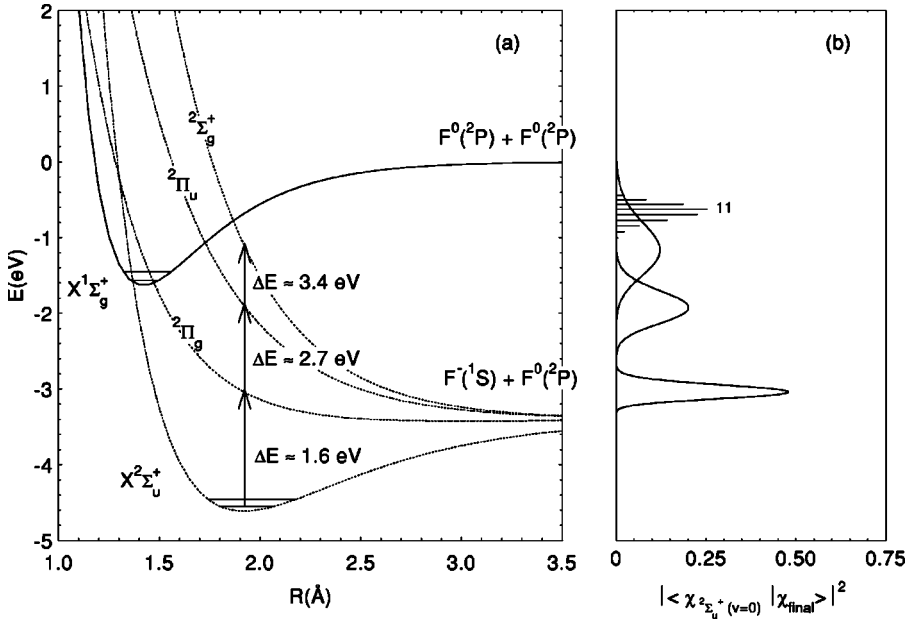


FIG. 1. (a) Potential-energy curves for the lowest electronic states of $F_2^-$ (dashed lines) and the ground state of $F_2^0$ (solid line). These potential-energy curves are Morse potential-energy curves obtained from experimental data as derived by Chen and Wentworth [34]. The vertical arrows illustrate transitions from the ground state to the dissociating curves. (b) Matrix elements of the nuclear wave functions of the ground state ($X\ ^2\Sigma_u^+$) of $F_2^-$ with the nuclear wave functions of the repulsive curves of symmetry $^2\Pi_g$, $^2\Pi_u$, $^2\Sigma_g^+$ (curves) and the ground state ($X\ ^1\Sigma_g^+$) of $F_2^0$ (lines) [35]. The size of the bound-continuum overlap matrix elements have been reduced by a factor of 250.

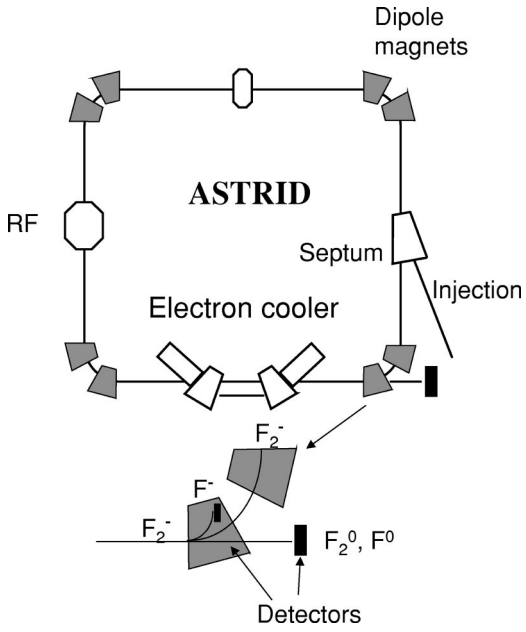


FIG. 2. Schematic drawing of the experimental setup at the ASTRID storage ring.

electron-ion collision process were detected (see Fig. 2). The ion current used for normalization was estimated from the induced voltage on an electrostatic pickup electrode in the ring.

The distribution of relative velocities is mainly determined by the electron velocity distribution, $f(v)$, and the accessible physical quantity is the rate coefficient

$$\langle v\sigma\rangle = \int v\sigma(v) f(v) dv, \tag{2}$$

which is the velocity weighted cross section. The electron velocity distribution in the rest frame of the ions is described by a flattened Maxwellian function centered on the detuning velocity $\Delta = |v_i - v_e|$ between ions and electrons [38]:

$$f(v) = \frac{m}{2\pi k T_\perp} e^{-m v_\perp^2/2kT_\perp} \sqrt{\frac{m}{2\pi k T_\parallel}}\, e^{-m(v_\parallel - \Delta)^2/2kT_\parallel}, \tag{3}$$

where $v_\perp$ and $v_\parallel$ are the electron velocity components perpendicular and parallel, respectively, to the ion-beam direction in the rest frame of the ions (the relative energy is $E = 1/2m(v_\perp^2 + v_\parallel^2)$). A low longitudinal temperature $kT_\parallel \sim 0.5 - 1.0$ meV [38] is obtained by the compression of the longitudinal electron velocity distribution due to the electron acceleration. The transverse temperature is the cathode temperature reduced by the technique of adiabatically expanding the electron beam [39] in a decreasing magnetic field; here $kT_\perp \sim 20$ meV. The distribution in relative energy is well-approximated by a Gaussian distribution of width $\delta E = 1/2kT_\parallel + kT_\perp + (2kT_\parallel E_0)^{1/2}$, where $E_0 = 1/2m\Delta^2$ is the detuning energy. The transverse temperature determines the energy resolution at low energies ($<1$ eV), while at higher energies the longitudinal temperature is the more important. For $E > kT_\perp$, the cross sections are to a good approximation given by $\sigma = \langle v\sigma\rangle/\Delta$.

In terms of experimentally determined quantities, the rate coefficient for a process leading to an event of type $X$, where $X$ is one of the channels ($F_2{}^0/F^0 + F^0$, $F^0$, or $F^-$), is given by

$$\langle v\sigma\rangle = \frac{R(X) - R_0(X) f}{F(F_2^-)} \frac{v_i}{L\varepsilon_d \rho_e}, \tag{4}$$

where $R(X)$ is the measured rate when the electron beam is turned on, $R_0(X)$ is the corresponding rate when the electron beam is turned off, $R(F_2{}^-)$ is the rate of ions entering the interaction region, $L$ is the effective length of the interaction region, $\varepsilon_d (=1)$ is the detector efficiency, and $\rho_e$ is the electron density. The factor $f$ corrects for the effect that $R(X)$ is measured a little later than $R_0(X)$ by the chopping technique. In the toroid regions, where the electron beam bends to merge and separate from the ion beam, the beams are not strictly parallel and the relative energies are different from the one in the straight section. The contributions from the toroid regions are subtracted from the measured cross sections by an iterative analysis procedure.

The major uncertainty of the absolute cross sections is associated with the ion-current measurement. The relative cross sections are subject to smaller uncertainties. In consequence, an absolute cross section was measured at a fixed energy while the cross sections as a function of energy were measured relative to this absolute value.

The surface barrier detector measures the energy deposited in the silicon material during the stopping of the incoming particles. Hence, detachment events leading either to a one-particle product ($F_2{}^0$) or a simultaneous two-particle product ($F^0 + F^0$) cannot be directly distinguished by the detector. To surpass this problem, we used a method where a grid of known transmission $T$ was inserted in front of the detector [24]. The rate of events with the fractional ($R_1$) and the full ($R_2$) energy, corresponding to detection of one $F^0$ or two $F^0$, respectively, is related to the cross sections for detachment ($\sigma_{F_2{}^0}$ and $\sigma_{F^0+F^0}$) and dissociation leading to one neutral fragment ($\sigma_{F^0}$) in the following way:

$$R_1(T) = \frac{1}{N(T)}[T\sigma_{F^0} + 2T(1-T)\sigma_{F^0+F^0}],$$
$$R_2(T) = \frac{1}{N(T)}(T\sigma_{F_2{}^0} + T^2\sigma_{F^0+F^0}), \tag{5}$$

where $T$ is the grid transmission and $N(T)$ is a normalization factor. These equations were solved to yield the branching ratio

$$R = \frac{\sigma_{F_2{}^0}}{\sigma_{F_2{}^0} + \sigma_{F^0+F^0}}. \tag{6}$$

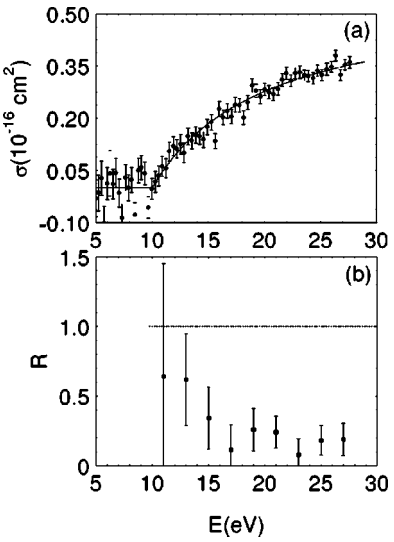


FIG. 3. (a) Absolute cross section for electron-impact detachment of $F_2^-$ leading to either a molecular fragment ($F_2^0$) or two atomic fragments ($F^0+F^0$). The solid line shows a fit to the cross section with a model cross section $\sigma=\sigma_0(1-E_{th}/E)$, giving $\sigma_0=0.55\times10^{-16}$ cm$^2$ and $E_{th}=10.0$ eV. (b) Ratio ($R$) of detachment leading to a molecular fragment in the final state relative to the total detachment cross section.

### III. RESULTS AND DISCUSSION

Figure 3(a) shows the total detachment cross section (final $F_2^0$ or $F^0+F^0$) while Fig. 3(b) shows the ratio $R$. The total detachment cross section is well-represented by the formula $\sigma=\sigma_0(1-E_{th}/E)$, with $\sigma_0=0.55\times10^{-16}$ cm$^2$ and $E_{th}=10.0$ eV as also shown in Fig. 3(a). The experimental threshold for detachment is seen to be in excess of the electron affinity of $F_2^0$ (3.08 eV) [40] by a factor of $\sim3.3$, which is larger than expected from the trend found in an earlier study of electron detachment from diatomic molecular anions [26] where a linear relation $E_{th}=2.2A+0.27$ eV was found. However, also $O_2^-$ showed a similar divergence from the main tendency. The shape of the detachment cross section compares well with the detachment cross section for other anions [25,26]. The branching ratio [Fig. 3(b)] decreases from a level being in favor of detachment into a molecular fragment near threshold to a level of $\sim20\%$ for energies higher than $\sim17$ eV. This behavior is very different from other molecular anions where detachment into an undissociated molecular fragment is the dominant reaction [26].

Except for the zero-point vibrational energy, the threshold for detachment plus dissociation is $D_e(F_2^-)+\mathrm{EA}(F^0)=1.26$ eV [34]$+3.40$ eV [40]$=4.66$ eV, which is also smaller than the experimental threshold of $10\pm0.5$ eV. Probably, detachment plus dissociation proceeds by vertical transitions to repulsive potential-energy curves of the neutral molecule as suggested for other molecular anions [26]. To the best of our knowledge the dissociative states of $F_2^0$ have never been investigated neither experimentally nor theoretically. However, from the Wigner-Witmer rules [41], potential-energy curves of symmetry $^1\Sigma_g^+(2)$, $^1\Sigma_u^+$, $^1\Pi_g$, $^1\Pi_u$, $^1\Delta_g$, $^3\Sigma_g^+$, $^3\Sigma_g^-$, $^3\Pi_g$, and $^3\Delta_u$ are expected to converge to the atomic limit $F^0(^2P)+F^0(^2P)$, thus, providing possible potential-energy curves by which the detachment plus dissociation can occur.

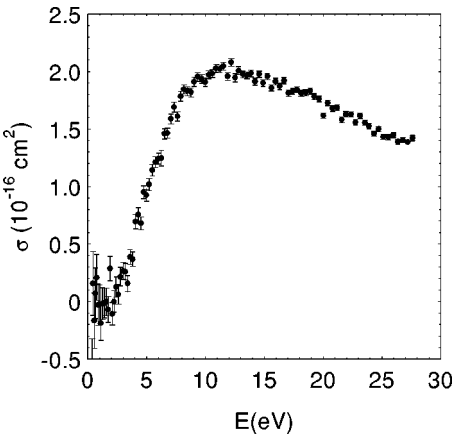


FIG. 4. Absolute cross section for electron-impact dissociation of $F_2^-$ obtained by detection of a single $F^0$.

In Fig. 4, the measured cross section for electron-impact dissociation of $F_2^-$ is shown (detection of $F^0$). An absolute cross section of $(1.9\pm0.6)\times10^{-16}$ cm$^2$ was measured at 15 eV. This cross section exhibits a threshold at $2.2\pm0.5$ eV after which it rises to a maximum near 12 eV. We also measured the cross section for dissociation leading to a negative particle in the final state. This cross section (not shown) is identical within the statistical error to the cross section for dissociation leading to a neutral particle in the final state except for a factor of 0.6, due to the fact that the charged fragment detector is too small to measure all $F^-$ ions from the interaction region. The two independent measurements together show that electron-impact dissociation (final $F^0+F^-$) does indeed give the dominanting contribution to this cross section, i.e., other dissociative reactions (final $F^-+F^+$ or final $F^0+F^+$) are unimportant at these energies.

The dissociation energy [34] of $F_2^-$ ($D_e=1.26$) is lower than the experimentally observed threshold of $2.2\pm0.5$ eV for electron-impact dissociation. The vertical excitation energies to the dissociating states of symmetry $^2\Pi_g$, $^2\Pi_u$, $^2\Sigma_g^+$ are $\sim1.6$ eV, $\sim2.7$ eV, and $\sim3.4$ eV, respectively [34], as marked in Fig. 1. The beam of $F_2^-$ is expected to exhibit a distribution of rovibrational states reflecting the temperature (1500 K) in the ion source. The initial rovibrational excitation remains during the ion storage, since rovibrationally excited molecules will not decay by radiative emission because the dipole moment is zero for homonuclear diatomic molecules. Rovibrationally excited states in the beam would, however, lower the experimental threshold. Thus, the data are in favor of a dissociation mechanism involving vertical excitation to the dissociating states of the anion. From the present experimental data it is impossible to point out through which of the three repulsive curves the reaction primarily proceeds.

In a comparison to previously studied atomic ($H^-$,$D^-$,$B^-$,$O^-$) [10–13] and homonuclear molecular anions [24–26] ($B_2^-$,$C_2^-$,$O_2^-$) the results obtained with $F_2^-$

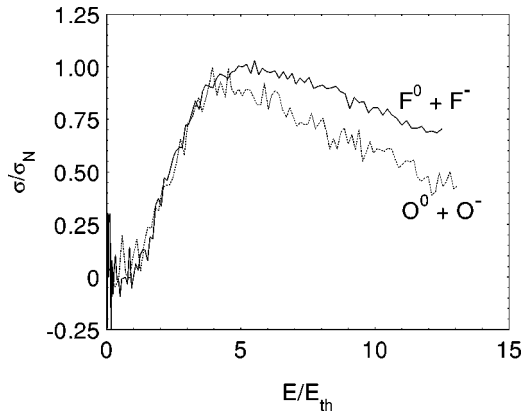


FIG. 5. Comparison of the dissociation cross section [26] for $F_2^-$ and $O_2^-$. The energy axis was normalized to the experimentally observed threshold while the cross section has been normalized to facilitate a comparison of the cross sections in the threshold region.

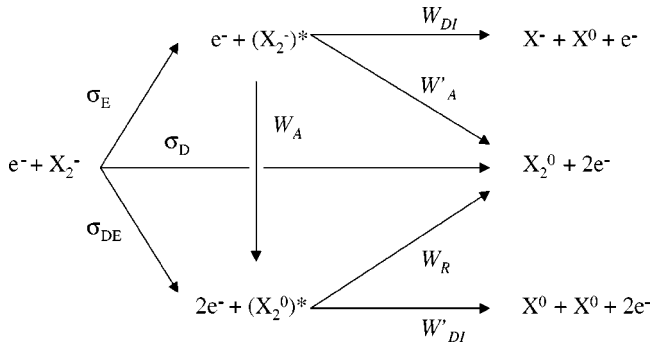


FIG. 6. Simplified illustration of the reaction pathways in electron molecular anion collisions. $\sigma$ is used as a symbol of scattering cross section while $W$ is used for the transition probability from an intermediate state to a given final state. The indices are $A$=autodetachment, $D$=direct detachment, DE=detachment and electronic excitation, DI=dissociation, $E$=electronic excitation, and $R$=radiative transition.

display both similarities and differences. The shapes of the various cross sections as a function of energy are similar for atomic and molecular anions. This was observed for nonresonant detachment and detachment plus dissociation reactions in Ref. [26]. While the cross sections for dissociation of $B_2^-$ and $C_2^-$ showed peak structures, which were attributed to the formation of dianions, the dissociation cross section of $O_2^-$ displayed a smooth behavior. In Fig. 5, the dissociation cross section for $F_2^-$ is compared to the previously measured dissociation cross section for $O_2^-$ [26]. The energy axis has been normalized to the experimentally observed thresholds and the cross sections have been normalized to facilitate a comparison of the cross sections in the threshold region. Presented in this way, the dissociation cross section for $O_2^-$ and $F_2^-$ are almost superimposable in the threshold region while a minor divergence is seen at higher energies. The similar shape of these cross sections suggests a general nonresonant mechanism for dissociation ($X^- + X^0, X = \mathrm{O,F}$).

Three main differences are observed when the cross sections for $F_2^-$ are compared to the measured cross section for other homonuclear anions ($B_2^-$, $C_2^-$, and $O_2^-$). Firstly, the measured effective threshold for detachment is higher than predicted from the trend found for other anions [26]. Secondly, above threshold the detachment plus dissociation is favored relative to pure detachment. Thirdly, the absolute cross section for dissociation is two orders of magnitude larger than that observed for other diatomic anions [26,42]. $O_2^-$ also showed a detachment threshold higher than predicted by the general tendency [26]. $O_2^-$ and $F_2^-$ both display an unfavorable overlap of the nuclear wave functions in the lower vibrational states of the neutral and anionic systems, which is evident by comparing the equilibrium distances in Table I, and it seems evident that an unfavorable overlap of the nuclear wave functions raises the detachment threshold. However, as seen from Fig. 1, electron detachment through a direct vertical transition to a vibrational excited level of $F_2^0$ ($^1\Sigma_g^+$) is indeed possible when considering only the overlap of the nuclear wave functions, the most favorable overlap being to the vibrational level $v = 11$ with a vertical energy difference of about 4 eV. For $F_2^-$, the threshold for electron detachment becomes in reasonable agreement with the tendency found for other anions if the vertical electron affinity is considered as the effective electron affinity.

The differences between the results obtained with $F_2^-$ and other anions can be explained by the lack of autodetachment after electronic excitation for $F_2^-$. Generally, electron detachment happens on the time scale of the electronic motion ($\sim 10^{-16} - 10^{-15}$ s) while dissociation happens on the time scale of the nuclear motion ($\sim 10^{-14}$ s). Hence, if autodetachment and dissociation are in free competition, the main flux will go to detachment rather than dissociation. As seen from the calculations of nuclear matrix elements in Fig. 1 for the ground vibrational level of $F_2^-$, transitions to the repulsive $F_2^-$ curves are most favorable where a subsequent autodetachment process is hindered by energy conservation. As a consequence, autodetachment is prevented after electronic excitation and the flux goes to dissociation. On the other hand, for $B_2^-$, $C_2^-$, and $O_2^-$ a vertical transition from the ground state to dissociative curves of the anion leaves the system with an energy that allows detachment reactions to compete with dissociation along the repulsive anionic curves and hence detachment is dominant. Thus, this suppression of autodetachment after electronic excitation can explain why the dissociation cross section is enhanced in $F_2^-$ relative to other anions. It is noted, however, that excitation to the $^2\Sigma_g^+$ repulsive curve of $F_2^-$ may result in autodetachment to the vibrational levels $v \geqslant 9$ of the electronic ground state of molecular $F_2^0$. The observation that detachment plus dissociation (final $F^0 + F^0$) is preferred to pure detachment (final $F_2^0$), while the opposite is true for other anions, can also be considered as an effect of the competition between autodetachment and dissociation after initial electronic excitation. While detachment plus dissociation primarily proceeds by direct transitions to repulsive curves of the neutral system and hence is unaffected by this competion, a major part of pure detachment may occur via initial elec-

tronic excitation followed by autodetachment and hence the actual yield of neutral molecules is highly sensitive to the dynamics of the repulsive anionic states.

In summary, Fig. 6 shows a schematic illustration of the nonresonant reaction pathways in electron collisions with molecular anions as revealed by our studies. The results obtained with $F_2^-$ emphasize that initial electronic excitation ($\sigma_E$) is an important process in electron anion scattering.

## IV. CONCLUSION

Collisions between free electrons and the molecular anion $F_2^-$ have been studied in a merged beams experiment at the heavy ion storage ring ASTRID. Absolute cross sections for detachment ($e^- + F_2^- \rightarrow F_2^0 + 2e^-$ or $F^0 + F^0 + 2e^-$) and dissociation ($e^- + F_2^- \rightarrow F^0 + F^- + e^-$) were measured in the energy range 0–27 eV. The branching between the two detachment channels was also studied. Dissociation is found to be the dominating reaction with a cross section that is an order of magnitude in excess of the total detachment cross section over most of the energy range studied. For both detachment and dissociation reactions, the shapes of the cross sections are similar to previously measured cross sections for other anions. The results obtained with $F_2^-$ are different from previously studied homonuclear anions on three main points, namely, (1) the experimental threshold for detachment is higher than expected from a general trend, (2) in detachment, the branching into a channel with a molecular fragment in the final state amounts to less than 20% over most of the energy range, and (3) the magnitude of the cross section for dissociation is about two orders of magnitude larger than observed for other anions. These observations may be understood by unfavorable overlaps of nuclear wave functions in the anionic and neutral systems and by the fact that autodetachment is hindered for some repulsive curves of $F_2^-$.

## V. ACKNOWLEDGMENTS

This work has been supported by the Danish National Research Foundation through the Aarhus Center for Atomic Physics (ACAP). We thank the ASTRID staff for support during the measurements.

[1] G. C. Tisone and L. M. Branscomb, Phys. Rev. Lett. **17**, 236 (1966).
[2] G. C. Tisone and L. M. Branscomb, Phys. Rev. **170**, 169 (1968).
[3] D. F. Dance, M. F. A. Harrison, and R. D. Rundel, Proc. R. Soc. London, Ser. A **299**, 525 (1967).
[4] B. Peart, D. S. Walton, and K. T. Dolder, J. Phys. B **3**, 1346 (1970).
[5] D. S. Walton, B. Peart, and K. T. Dolder, J. Phys. B **4**, 1343 (1971).
[6] B. Peart and K. T. Dolder, J. Phys. B **6**, 1497 (1973).
[7] B. Peart, R. A. Forrest, and K. T. Dolder, J. Phys. B **12**, 847 (1979).
[8] B. Peart, R. A. Forrest, and K. T. Dolder, J. Phys. B **16**, 2735 (1979).
[9] B. Peart, R. A. Forrest, and K. T. Dolder, J. Phys. B **12**, L115 (1979).
[10] T. Tanabe *et al.*, Phys. Rev. A **54**, 4069 (1996).
[11] L. H. Andersen, D. Mathur, H. T. Schmidt, and L. Vejby-Christensen, Phys. Rev. Lett. **74**, 892 (1995).
[12] L. H. Andersen, N. Djuric, M. J. Jensen, H. B. Pedersen, and L. Vejby-Christensen, Phys. Rev. A **58**, 2819 (1998).
[13] L. Vejby-Christensen, D. Kella, D. Mathur, H. B. Pedersen, H. T. Schmidt, and L. H. Andersen, Phys. Rev. A **53**, 2371 (1996).
[14] R. W. Hart, E. P. Gray, and W. H. Guier, Phys. Rev. **108**, 1512 (1957).
[15] E. A. Solov'ev, Zh. Eksp. Teor. Fix. **72**, 2072 (1977) [Sov. Phys. JETP **45**, 1089 (1978)].
[16] B. M. Smirnov and M. I. Chibisov, Zh. Eksp. Teor. Fiz. **49**, 841 (1965) [Sov. Phys. JETP **22**, 585 (1966)].
[17] V. N. Ostrovsky and K. Taulbjerg, J. Phys. B **29**, 2573 (1996).
[18] A. K. Kazansky and K. Taulbjerg, J. Phys. B **29**, 4465 (1996).
[19] J. T. Lin, T. F. Jiang, and C. D. Lin, J. Phys. B **29**, 6175 (1996).
[20] M. S. Pindzola, Phys. Rev. A **54**, 3671 (1996).
[21] P. V. Grujic and N. Simonovic, J. Phys. B **31**, 2611 (1998).
[22] J. M. Rost, Phys. Rev. Lett. **82**, 1652 (1999).
[23] F. Robicheaux, Phys. Rev. Lett. **82**, 707 (1999).
[24] L. H. Andersen, P. Hvelplund, D. Kella, P. H. Mokler, H. B. Pedersen, H. T. Schmidt, and L. Vejby-Christensen, J. Phys. B **29**, L643 (1996).
[25] H. B. Pedersen, N. Djuric, M. J. Jensen, D. Kella, C. P. Safvan, H. T. Schmidt, L. Vejby-Christensen, and L. H. Andersen, Phys. Rev. Lett. **81**, 5302 (1998).
[26] H. B. Pedersen, N. Djuric, M. J. Jensen, D. Kella, C. P. Safvan, H. T. Schmidt, L. Vejby-Christensen, and L. H. Andersen, Phys. Rev. A **60**, 2882 (1999).
[27] R. D. Mead, U. Hefter, P. A. Schulz, and W. C. Lineberger, J. Chem. Phys. **82**, 1723 (1985).
[28] M. J. Travers, D. C. Cowles, and G. B. Ellison, Chem. Phys. Lett. **164**, 449 (1989).
[29] K. P. Huber and G. Herzberg, *Molecular Structure and Molecular Spectra. IV. Constants of Diatomic Molecules* (Van Nostrand Reinhold, New York, 1979).
[30] H. Patridge, C. W. Bauschlicher Jr., S. R. Langhoff, and P. R. Taylor, J. Chem. Phys. **95**, 8292 (1991).
[31] T. G. Slanger and P. C. Cosby, J. Phys. Chem. **92**, 267 (1988).
[32] *Atomic Energy Levels*, edited by C. E. Moore, Natl. Bur. Stand. (U.S.) Circ. No. 467 (U.S. GPO, Washington, 1949), Vol. 1.
[33] P. J. Bruna and J. S. Wright, J. Phys. B **23**, 2197 (1990).
[34] E. C. M. Chen and W. E. Wentworth, J. Phys. Chem. **89**, 4099 (1985).
[35] The nuclear wave functions ($\chi$) used to evaluate the overlap matrix elements were obtained by numerically solving the

Schrödinger equation for the nuclear motion neglecting the effects of rotation. For the bound states, the vibrational wave functions were calculated using the matrix techniques described by P. J. Cooney, E. P. Kanter, and Z. Vager, Am. J. Phys. **49**, 76 (1981). The continuum wave functions were determined as energy normalized wave functions [see, for instance, E. Merzbacher, *Quantum Mechanics*, 2nd ed. (Wiley, New York, 1970), pp. 85–88 and 231–233], i.e.,

$$\chi(R,E) \rightarrow \sqrt{\frac{2\mu}{\pi k}} \cos[kR + \delta(E)] \quad \text{for} \quad R \rightarrow \infty,$$

where $\mu$ is the reduced mass, $k = (2\mu E)^{1/2}$, and $\delta(E)$ is a phase shift.

[36] S. P. Møller, in *Conference Record of the 1991 IEEE Particle Accelerator Conference: Accelerator Science and Technology, San Francisco, 1991*, edited by L. Lizama (IEEE, New York, 1991), p. 2811.

[37] P. Tykesson, H. H. Andersen, and J. Heinemeier, IEEE Trans. Nucl. Sci. **23**, 1104 (1976).

[38] L. H. Andersen, J. Bolko, and P. Kvistgaard, Phys. Rev. A **41**, 1293 (1990).

[39] H. Danard, Nucl. Instrum. Methods **A335**, 397 (1993).

[40] W. A. Chupka, J. Berkowitz, and D. Gutman, J. Chem. Phys. **55**, 2724 (1971).

[41] G. Herzberg, *Spectra of Diatomic Molecules* (van Nostrand, New York, 1950), Chap. VI, p. 321.

[42] An absolute detachment cross section for $O_2^-$ that was not given in Ref. [26] has been measured at ASTRID to be $2.83 \times 10^{-16}$ cm$^2$ at 15 eV, which gives a corresponding dissociation cross section of $7.5 \times 10^{-18}$ cm$^2$ at this energy.